PHYSICAL REVIEW B VOLUME 35, NUMBER 13 1 MAY 1987

# $^2$H NMR studies of structural phase transitions in some members of the deuterated $ABF_6\cdot 6H_2O$ system

M. Bose, K. Roy, and A. Ghoshray
*Saha Institute of Nuclear Physics, Calcutta-700 009, India*

(Received 15 October 1985; revised manuscript received 7 July 1986)

$^2$H NMR measurements in single crystals of deuterated $CoSiF_6\cdot 6H_2O$, $CoTiF_6\cdot 6H_2O$, and $ZnTiF_6\cdot 6H_2O$ in the temperature range 100–300 K reveal two successive phase transitions, in each case for the first time. The quadrupole coupling constants and the direction cosines of the principal electric-field-gradient tensors of the deuterons are determined at different phases. It has been found that above the first transition at $T_{c1}$ (which lies in the range 220–270 K) $^2$H NMR results in each case are consistent with rhombohedral ($R\bar{3}$) symmetry with unimolecular unit cells. Below the transition at $T_{c1}$, though the octahedra are found to be distorted (the extent of the distortion and the nature of the transition differs from member to member), the equivalency of the six water molecules is preserved in the unimolecular unit cell. The shape of the potential well of the O-H $\cdots$ F bond is found to alter significantly. The O-H bonds, which were parallel to the symmetry axis in the rhombohedral phase, are rotated by $\sim 6\pm 1°$ below the transition at $T_{c1}$, whereas those perpendicular to this axis are rotated by $\sim 3\pm 1°$. The transition at $T_{c2}$ (170–185 K) are sharply first order in nature and depend critically on the cooling rate. During this transition, the equivalency of the six water molecules is destroyed with the appearance of two types ($A$ and $B$) of water molecules in the ratio 2:1, along with a cell doubling. A small change (in comparison to the intermediate phase which lies in the range $T_{c1} > T > T_{c2}$) in the O-H directions of $A$-type molecules is observed, whereas for $B$ type this change is appreciable for both parallel and perpendicular bonds. The results further indicate that the transition at $T_{c1}$ is ferrodistortive in nature and is triggered in the water octahedra. However, the transition at $T_{c2}$ appears to be antiferrodistortive, involving a distortion in both water and fluorine octahedra and the structure is more compatible with monoclinic symmetry with $Z=2$.

## I. INTRODUCTION

The $ABF_6\cdot 6H_2O$ system (where $A = Fe^{2+}$, $Co^{2+}$, $Ni^{2+}$, $Zn^{2+}$, etc. and $B = Sn^{4+}$, $Si^{4+}$, $Ti^{4+}$, etc.) is of interest as most of the members exhibit structural phase transitions below 300 K which have been investigated by different macroscopic[1–4] and microscopic[5–9] methods. Though detailed structural data are available for the room-temperature phases of these compounds, the data for the low-temperature phases are in no way complete. At 300 K, the compounds belong to either the $R\bar{3}$ or $R\bar{3}m$ space groups[10] with $Z=1$. Basically the structure is composed of $[A(H_2O)_6]^{2+}$ and $(BF_6)^{2-}$ octahedra linked by the O-H $\cdots$ F bond and arranged in a trigonally distorted CsCl packing (Fig. 1). It has been suggested from x-ray studies that the space group of $MgSiF_6\cdot 6H_2O$ below the transition temperature [296 K (Ref. 11)] is $P2_1/c$ with $Z=2$ and $CoSiF_6\cdot 6H_2O$ around 160 K has a monoclinic structure[12] with $Z=2$.

EPR studies of the metal ion ($A$) at 300 K correspond to a single magnetic site, whereas the low-temperature spectra are not identical for different members. For example, $Mn^{2+}$-doped $CoSiF_6\cdot 6H_2O$ has two magnetically inequivalent sites[13] below $T_c$, whereas those for $Ni^{2+}$ in $ZnTiF_6\cdot 6H_2O$ ($T_c \sim 182$ K)[14] and $NiTiF_6\cdot 6H_2O$ has six.[6] This indicates that the deviation from axial symmetry in the low-temperature phase varies significantly from member to member.

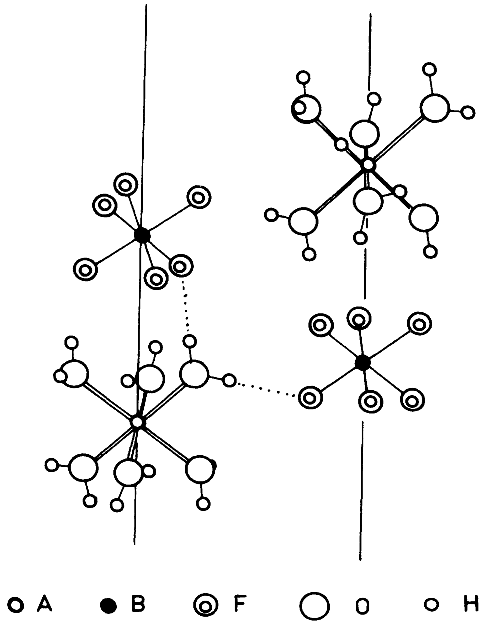

FIG. 1. Two neighboring columns in the structure of $ABF_6\cdot H_2O$ system.

Afanasyev *et al.*[15] have shown from $^{19}$F NMR studies that the transition in $ZnTiF_6 \cdot 6H_2O$ at 182 K is accompanied by the stoppage of the reorientational motion of $(TiF_6)^{2-}$ octahedra along with a tetragonal distortion resulting in two types of fluorine atoms in the ratio 2:1. Moreover, the Raman studies[8] indicate distortion of both $(TiF_6)^2$ and $[Ni(H_2O)_6]^{2+}$ octahedra in $NiTiF_6 \cdot 6H_2O$ along with a lowering of the lattice symmetry, whereas in $FeSiF_6 \cdot 6H_2O$ only the lattice symmetry is lowered.[7] Further the transition temperatures vary from member to member [246 K for $CoSiF_6 \cdot 6H_2O$,[1] 220 K for $MnTiF_6 \cdot 6H_2O$,[9] and 136 K for $NiTiF_6 \cdot 6H_2O$ (Ref. 8)]. Thus even in the isomorphous series of compounds belonging to the $ABF_6 \cdot 6H_2O$ system, nature of the transition can not be fitted to a simple physical model.

Thus in spite of the large amount of experimental data available, the phase transition in this system is not well understood. In particular, the role of the O-H $\cdots$ F bonds which link $[A(H_2O)_6]^{2+}$ and $(BF_6)^{2-}$ octahedra has not been elucidated. Study of these hydrogen bonds could provide useful information, as the effect of the distortion of one of the octahedra would be communicated to the other through these bonds. Information regarding the hydrogen bond may be obtained from either neutron diffraction or $^2$H NMR measurements. With this view in mind, a systematic $^2$H NMR study has been made in some deuterated members of this series. Henceforth, $^2$H NMR in any member of the $ABF_6 \cdot 6H_2O$ system will indicate deuteron magnetic resonance in the corresponding deuterated analogue of the hydrated crystal. The electric field gradient (EFG) at the $^2$H site arises mainly from the charge distribution in the hydrogen bond, so it is expected that $^2$H NMR monitored as a function of temperature would provide information about the change in the structure of the O-H $\cdots$ F bond associated with the phase transition. In the present study the quadrupolar interaction parameters viz., $e^2qQ/h$, $\eta$ and the direction cosines of the principal axes of the EFG tensors with respect to the crystal axes in the range 100–300 K reveal for the first time that deuterated $CoSiF_6 \cdot 6H_2O$, $CoTiF_6 \cdot 6H_2O$ and $ZnTiF_6 \cdot 6H_2O$ undergo structural phase transition from rhombohedral to monoclinic phase through an intermediate phase.

## II. EXPERIMENTAL

Fluorotitanates are prepared by adding freshly prepared metal carbonate to fluorotitanic acid. Fluorosilicic acid is used in the case of $CoSiF_6 \cdot 6H_2O$. Deuteration is performed by repeated recrystallization of the compound from 99.9% heavy water. Large hexagonal prism-shaped single crystals of deuterated (90%) compound, suitable for NMR experiment, with well developed $\{110\}$ and $\{1\bar{1}0\}$ prismatic faces, elongated along [111] direction are obtained.

The $^2$H NMR is observed at 7.0 and 15.0 MHz using a Varian Associates WL 210 nuclear induction spectrometer. The magnetic field is supplied using either a Varian Associates V4012A 12-in. or V7400 15-in. electromagnet. Investigations are made over the temperature range 100–300 K using a Varian variable-temperature accessory.

## III. RESULTS AND DISCUSSION

Interaction of the quadrupole moment of a $^2$H nucleus ($I=1$) with the EFG at the nuclear site results in a splitting of the resonance line. The angular dependence of the line pair separation, $2(\Delta\nu)$ for each deuteron in presence of the Zeeman field, $H_0$ is related to the EFG components $V_{ij}$ in the following manner[16]

$$2(\Delta\nu)_x = (3eQ/4h)[V_{xx} + (V_{zz} - V_{yy})\cos(2\theta_x) + 2V_{yz}\sin(2\theta_x)] \ . \quad (1)$$

Here $\theta_x$ is the angle between the crystal $y$ axis and the direction of the magnetic field. The components $V_{ij}$ are referred to the orthogonal set of axes $x$, $y$, and $z$ fixed in the crystal. All elements of the EFG tensor may be obtained by performing rotations about three orthogonal axes. In the present case, use is made of two nonorthogonal planes of rotation about $x$ and $x'$ axes as discussed in our earlier publications.[17,18] where we have reported $^2$H NMR results of $NiTiF_6 \cdot 6H_2O$ in the range 100–300 K and some preliminary results of $CoSiF_6 \cdot 6H_2O$, $CoTiF_6 \cdot 6H_2O$, and $ZnTiF_6$. $6H_2O$ in the range 210–300 K. The present paper deals with the $^2$H NMR results of $CoSiF_6 \cdot 6H_2O$, $CoTiF_6 \cdot 6H_2O$, and $ZnTiF_6 \cdot 6H_2O$ in the range 100–300 K and a comparison with those of $NiTiF_6 \cdot 6H_2O$.

At 300 K, in each case we have obtained three distinct EFG tensors corresponding to three $H_2O$ molecules which are transformed to each other by the $\bar{3}$ axis (this axis lies along the crystallographic $c$ axis). Results are consistent with $R\bar{3}$ symmetry with $Z=1$. Further, the total number of $^2$H lines and the principal EFG tensors reveal that each deuteron in a water molecule undergoes a fast ($\gg 10^6$ Hz) 180° flip motion about the bisectrix of the *H-O-H* bond angle. The flipping frequency, $\nu_f$ being temperature dependent affects the line width $\delta\nu$. For the very fast motion, where $\nu_f \gg \nu_R$ ($\nu_R$ is the Larmor frequency of $^2$H), dipolar contribution to $\delta\nu$ reduces considerably resulting in a narrower resonance line. Furthermore, in this fast motion region, the deuterons in a water molecule experience the same average EFG resulting in a single pair of line for the two deuterons. With lowering of temperature $\nu_f$ slows down and in the limit $\nu_f \sim \nu_R$, dipolar contribution predominates and broadening of the resonance line occurs. Ultimately in a temperature region where $\nu_f \sim \nu_1 - \nu_2$ (difference in quadrupolar splitting frequency of the two deuterons in a water molecule) the lines are not detectable, because they smear out over the whole frequency range $\nu_1 - \nu_2$. Finally, when $\nu_f \ll (\nu_1 - \nu_2)$, the lines should again reappear with the total number of $^2$H lines being doubled as compared to the fast motion region. All these features are observed in all the members during the $^2$H NMR investigation. In general, $^2$H lines are not detectable from 190–200 K. The reappearance of the $^2$H lines have been detected for $CoSiF_6 \cdot 6H_2O$ and $CoTiF_6 \cdot 6H_2O$ around 190 K and for $NiTiF_6 \cdot 6H_2O$ at 160 K. For $ZnTiF_6 \cdot 6H_2O$, the lines have been detected below

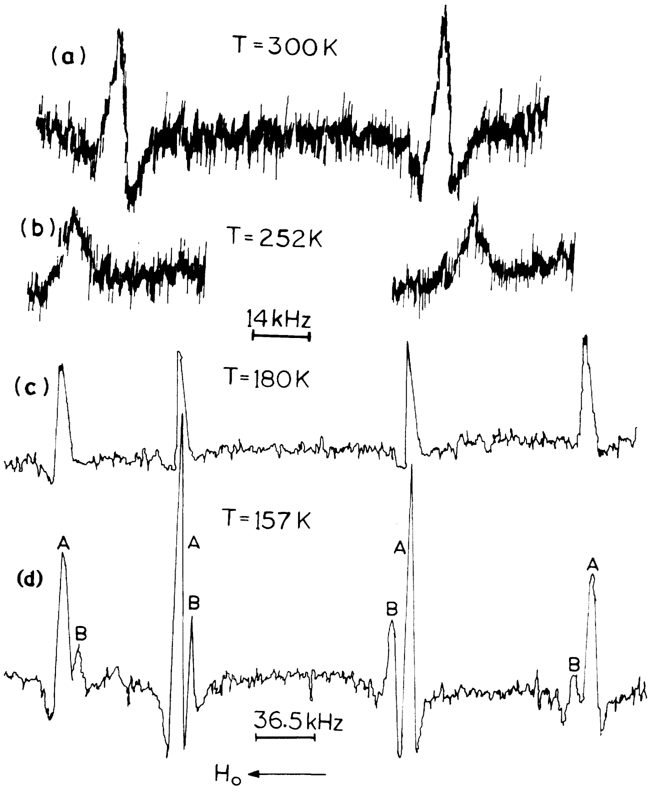

FIG. 2. $^2$H NMR spectra of $CoSiF_6 \cdot 6H_2O$ at $\theta_x = 90°$ ($c \| H_0$). (a) $T=300$ K, (b) $T=252$ K, (c) $T=180$ K, and (d) $T=157$ K: $\nu_R = 7.0$ MHz for (a) and (b); $\nu_R = 15.0$ MHz for (c) and (d).

160 K using a digital signal analyzer (Tracor Northern NS570A). Figures 2(a) and 2(c) show $^2$H NMR spectra of $CoSiF_6 \cdot 6H_2O$ at the orientation $\theta_x = 90°$ with $H_0$ parallel to the $z$ axis ($z$ axis of the crystal fixed frame is along the crystallographic $c$ axis) at 300 and 180 K corresponding to fast and slow motion region, respectively. In this orientation at 300 K, three pairs of lines corresponding to three water molecules per unit cell (other three are related by the inversion symmetry) coalesce into a single pair. Due to motional average of the EFG as described earlier, the lines for two deuterons in a water molecule remain unresolved. At 180 K, two deuterons in a water molecule experience different EFG and as such two pairs of lines appear instead of a single pair. We shall now discuss in the following two subsections the $^2$H NMR results in the light of structural phase transition.

### A. $^2$H NMR in the range 200–300 K

Figures 3 and 4 show the line pair separation, $2(\Delta\nu)_x$ and the line width, ($\delta\nu$) of the individual line, respectively, as a function of temperature at the orientation $\theta_x = 90°$ [cf. Figs. 2(a) and 2(b)]. For $NiTiF_6 \cdot 6H_2O$, $2(\Delta\nu)$ remains constant throughout the range. However, $\delta\nu$ increases continuously with lowering of temperature. This change in $\delta\nu$ is found to fit with the relation

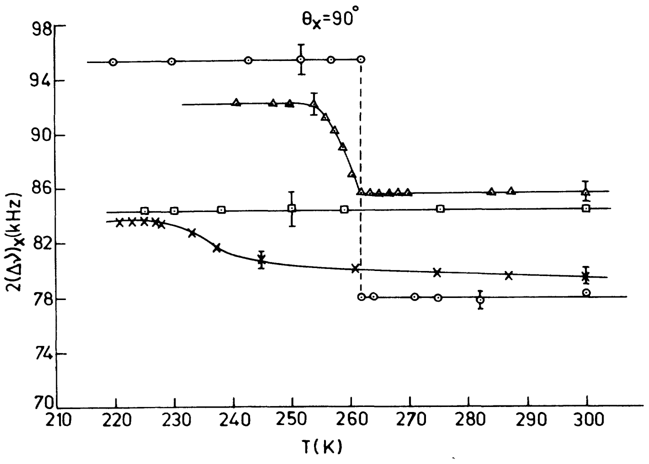

FIG. 3. Temperature dependence of the quadrupolar splitting frequency, $2(\Delta\nu)_x$ of $^2$H resonance at 7.0 MHz: ⊙, $CoSiF_6 \cdot 6H_2O$; △, $CoTiF_6 \cdot 6H_2O$; □, $NiTiF_6 \cdot 6H_2O$; and ×, $ZnTiF_6 \cdot H_2O$.

$$\delta\nu = \delta\nu_0 + \tfrac{1}{2}\pi^2[(\nu_1 - \nu_2)^2/\nu_f] , \tag{2}$$

where $\delta\nu_0$ is the rigid lattice dipolar width and $\nu_f$ is the flipping frequency of the water molecule. Knowing $\nu_f$ from Eq. (2), we have determined the potential barrier, $V_0$ for such motion by assuming Arrhenius equation

$$\nu_f = \nu_0 \exp(-V_0/RT) .$$

The value of $V_0$ in this case is found to be 6.0 kcal/mole and is close to the energy normally required to break the hydrogen bond. This behavior is very general in the hydrate crystals. However, other three members exhibit similar anomaly both in $2(\Delta\nu)$ and $\delta\nu$ (Figs. 3 and 4) which we have associated with the structural phase transi-

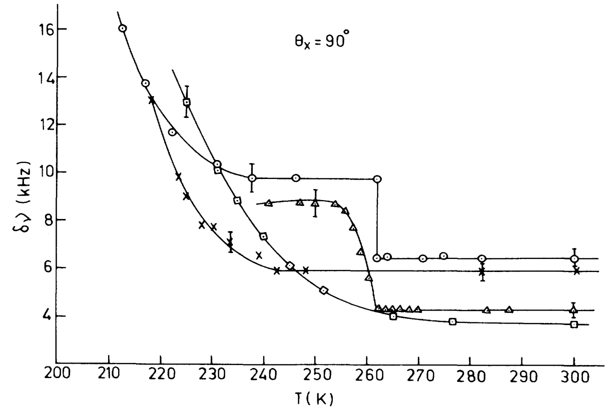

FIG. 4. Temperature dependence of line width, $\delta\nu$ (peak-to-peak separation of the derivative of an absorption line) of $^2$H resonance in ⊙, $CoSiF_6 \cdot 6H_2O$; △, $CoTiF_6 \cdot 6H_2O$; □, $NiTiF_6 \cdot 6H_2O$; and × $ZnTiF_6 \cdot H_2O$.

TABLE I. Principal components and their direction cosines for the EFG tensors of deuterons in $CoSiF_6 \cdot 6H_2O$ at $T = 180$ K.

| Tensor | Deuteron | $e^2Qq_{ii}/h$ (kHz) | Direction cosines with respect to crystallographic axes | | |
|---|---|---|---|---|---|
| | | | $x$ | $y$ | $z$ |
| I | $D_1$ | 111.4 | 0.3862 | −0.9152 | −0.1150 |
| | | 132.4 | 0.8948 | 0.4019 | −0.1943 |
| | | −243.8 | 0.2241 | −0.0278 | 0.9742 |
| II | $D_3$ | 111.1 | −0.6238 | 0.7781 | 0.0742 |
| | | 136.0 | 0.7698 | 0.5952 | 0.2303 |
| | | −247.1 | −0.1349 | −0.2008 | 0.9703 |
| III | $D_5$ | 112.4 | −0.4319 | 0.8673 | −0.2473 |
| | | 130.7 | 0.8940 | 0.4479 | 0.0096 |
| | | −243.1 | −0.1191 | 0.2170 | 0.9689 |
| IV | $D_2$ | −103.8 | −0.1963 | −0.2593 | 0.9456 |
| | | −127.7 | 0.0666 | 0.9586 | 0.2766 |
| | | 231.5 | 0.9783 | −0.1173 | 0.1709 |
| V | $D_4$ | −102.5 | −0.0657 | 0.2498 | 0.9661 |
| | | −129.3 | 0.7884 | −0.5804 | 0.2037 |
| | | 231.8 | 0.6116 | 0.7751 | −0.1588 |
| VI | $D_6$ | −102.4 | 0.4918 | 0.0392 | 0.8698 |
| | | −125.2 | 0.7883 | 0.4042 | −0.4639 |
| | | 227.6 | −0.3698 | 0.9138 | 0.1679 |

tions ($T_{c1}$). The variation of $\delta\nu$ with temperature in these cases cannot be fitted with the simple Eq. (2). Well below the transition at $T_{c1}$ effect of the motional broadening predominates in $\delta\nu$. The similar behavior of $2(\Delta\nu)$ and $\delta\nu$ near the transition at $T_{c1}$ clearly reveal that the shape of the potential well of the O-H $\cdots$ F bond, is altered. This is plausible because such a change would modify the barrier for 180° flip motion of $H_2O$ and hence $\nu_f$ and also the EFG at the $^2H$ site simultaneously.

It is interesting to note that the $^2H$ NMR spectra below the transition at $T_{c1}$ in the three members are identical in nature; although the order of transition is different for different members as revealed from the variation of $2(\Delta\nu)$ and $\delta\nu$. Figure 2(b) shows the $^2H$ NMR spectra of $CoSiF_6 \cdot 6H_2O$ at $\theta_x = 90°$ below the transition at $T_{c1}$; which shows that all the $H_2O$ molecules are still equivalent. Further, it has been observed that the total number of lines at an arbitrary orientation remain the same below the transition at $T_{c1}$. Thus, the present results do not give any evidence of cell doubling below the transition at $T_{c1}$. Previously this transition was assumed to be associated with a cell doubling.[14] Therefore, this phase needs further investigation. A systematic rotation pattern can provide information about the nature of the transition as well as a picture of the hydrogen bond network in this phase. Due to excessive line broadening below the transition at $T_{c1}$, the signal-to-noise ratio (S/N) prohibits detailed rotation pattern in this temperature range. So we have to do this near 180 K where comparatively narrow lines corresponding to slower flip motion are observed.

### B. $^2H$ NMR in the range 100–200 K

Reappearance of $^2H$ lines in case of $CoSiF_6 \cdot 6H_2O$ and $CoTiF_6 \cdot 6H_2O$ occur near 190 K and around 160 K (Ref. 18) for $NiTiF_6 \cdot 6H_2O$. Figure 2(c) shows the NMR spectrum at 180 K in $CoSiF_6 \cdot 6H_2O$ at $\theta_x = 90°$. Instead of a single pair of lines which disappeared around 200 K, there appear two pairs of lines corresponding to two deuterons in a water molecular due to the reason mentioned earlier. As the NMR spectra of $CoSiF_6 \cdot 6H_2O$ and $CoTiF_6 \cdot 6H_2O$ are very similar, the results of detailed rotation pattern will be given only for $CoSiF_6 \cdot 6H_2O$.

The rotation pattern about the $x$ axis (Fig. 5) depicts maximum six pairs of lines corresponding to six deuterons belonging to three water molecules. The $^2H$ lines for the other three water molecules out of the six per unit cell still remain indistinguishable as it was at 300 K. This result indicates that even below the transition at $T_{c1}$, the center of inversion of the crystal exists and the unit cell still remain unimolecular. Principal EFG tensors for the six deuterons are given in Table I. Since we have no knowledge about the atomic coordinates of the phase below the transition at $T_{c1}$, it is not possible to use the empirical rule of Soda and Chiba[19] for assignment of deuterons belonging to a particular hydrogen bond. However, we have assigned them by comparing the $^2H$ NMR spectra of $CoSiF_6 \cdot 6H_2O$ at 180 K with those of $NiTiF_6 \cdot 6H_2O$ at 150 K (Ref. 18) (where this system is in $R\bar{3}$ phase). This has been checked further by comparing the direction cosines of the $z$ principal axis ($z_p$) of the deuterons, with the O-H directions calculated by using the

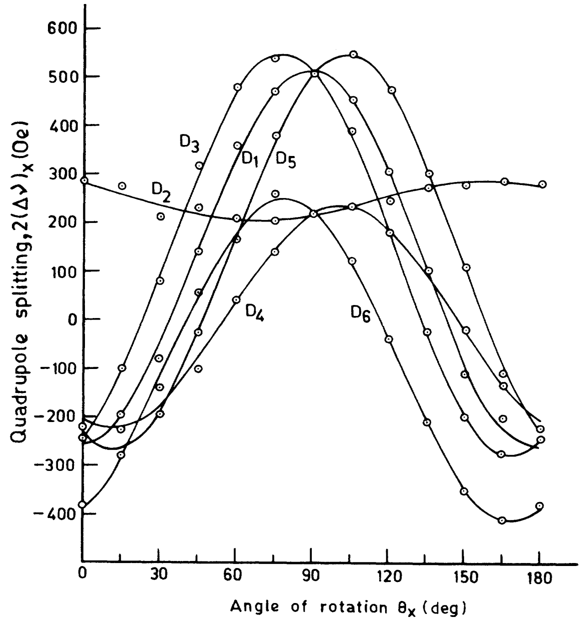

FIG. 5. Angular dependence of $^2$H line splitting, $2(\Delta\nu)_x$ about $x$ axis in $CoSiF_6\cdot6H_2O$ at 180 K; curves are least-squares fit of the experimental data.

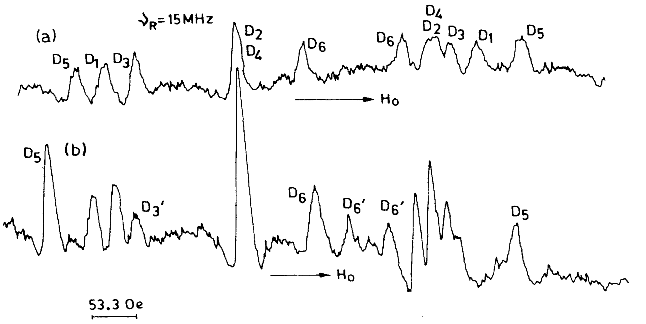

FIG. 6. $^2$H NMR spectra of $CoSiF_6\cdot6H_2O$ at $\theta_x = 105°$ for $x$ rotation: (a) $T = 180$ K and (b) $T = 140$ K at $\nu_R = 15.0$ MHz.

atomic coordinates of $CoSiF_6\cdot6H_2O$ given for the $R\bar{3}$ phase. The deviation, $\delta\theta_z$ of the $z_p$ direction (i.e., the O-H direction) from the calculated O-H direction corresponding to $R\bar{3}$ phase are given in Table II. The deviation $\delta\theta_y$ of the $y$ principal axis, $y_P$ from the calculated $y_P$ direction [normal to the Co-O-H plane (Ref. 19)] of the $R\bar{3}$ phase has also been included. Appreciably large values of $\delta\theta_y$ compared to $\delta\theta_z$ indicate that the transition at $T_{c1}$ do not alter the O-H directions appreciably. However, it changes the potential surface of the O-H $\cdots$ F bond significantly and hence affects the barrier for the 180° flip motion of $H_2O$. As a consequence the flipping frequency, $\nu_f$ is also changed affecting the line width at the transition at $T_{c1}$, as observed in the present case (Fig. 4). These results further indicate that the transition at $T_{c1}$ is of ferrodistortive in nature, keeping the total number of molecules per unit cell unchanged.

On further lowering of temperature, $CoSiF_6\cdot6H_2O$ and $CoTiF_6\cdot6H_2O$ exhibit a second phase transition at 170±2 K and 175±2 K, respectively, which would be designated as $T_{c2}$. In each case, the transition is sharply first order in nature. It has been observed that the cooling rate is very critical in the detection of transition at $T_{c2}$. We have to cool the crystal at a rate of 1 K/min. Figure 2(d) shows the NMR spectra of $CoSiF_6\cdot6H_2O$ below the transition at $T_{c2}$ at $\theta_x = 90°$. It is seen that each resonance line [cf. Fig. 2(c)] splits into two in the intensity ratio 2:1. This clearly reveals that due to this transition the crystal symmetry is lowered to such an extent that the equivalency of six $H_2O$ molecules is destroyed with the appearance of two types of water molecules, viz., $A$ and $B$ in the ratio 2:1. Further, a comparison of the NMR spectra for the orientation $\theta_x = 105°$ at above and below the transition at $T_{c2}$ (Fig. 6) shows that new lines such as $D_6$ and $D_3$ appear and the position of the $D_5$ line changes in the phase below the transition at $T_{c2}$. Figure 7 shows the rotation pattern of $CoSiF_6\cdot6H_2O$ about $x$ axis at 140 K. In this phase the maximum number of $^2$H lines that appear at a particular orientation $\theta_x = 120°$ is nine. The intensities and widths of the different lines differ considerably, indicating that all the $^2$H lines are not resolved.

However, it has been found that some of the lines which are unresolved at a particular orientation, are

TABLE II. Electric quadrupole coupling constant $e^2Qq/h$, asymmetry parameter, $\eta$ and angle $\phi_z$ between the $z$ principal axes of two deuterons belonging to a $H_2O$ molecule of $CoSiF_6\cdot6H_2O$ at 180 K.

| Assignment | | $e^2Qq/h$ (kHz) | Asymmetry parameter $\eta$ | $\delta\theta_z$ [a] (deg) | $\delta\theta_y$ [b] (deg) | Mean value of $\phi_z$ (deg) |
|---|---|---|---|---|---|---|
| $O_I$ | $D_1$ | −243.8±2.0 | 0.086±0.02 | 5.0±1.5 | 18.1±2 | |
| | $D_2$ | 231.3±2.0 | 0.104±0.02 | 3.8 | 28.1 | |
| $O_{II}$ | $D_2$ | −247.1±2.0 | 0.101±0.02 | 7.7 | 1.9 | 112±1 |
| | $D_4$ | 231.8±2.0 | 0.116±0.02 | 2.2 | 31.5 | |
| $O_{III}$ | $D_5$ | −243.1±2.0 | 0.075±0.02 | 7.2 | 16.1 | |
| | $D_6$ | 227.6±2.0 | 0.100±0.002 | 2.8 | 18.2 | |

[a] $\delta\theta_z$ is the change in O-H direction as defined in the text.
[b] $\delta\theta_y$ is the change in the $y_p$ direction as defined in the text.

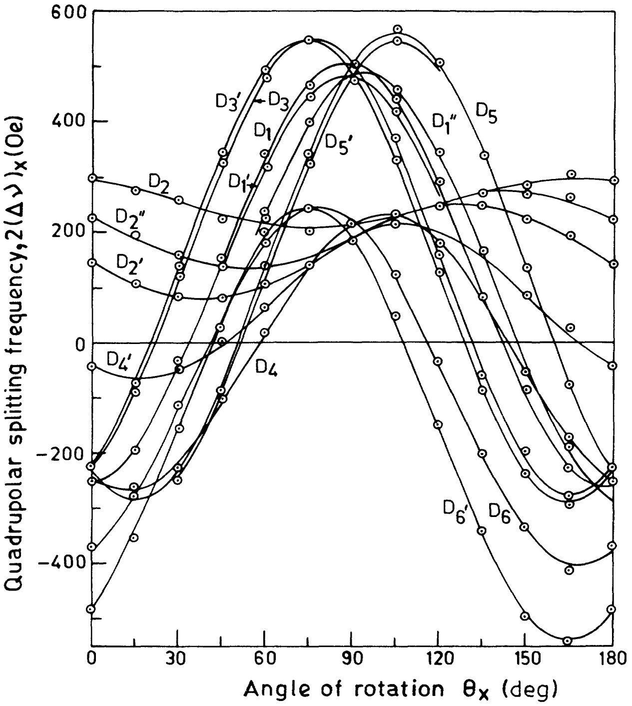

FIG. 7. Angular dependence of $^2$H line splitting, $2(\Delta\nu)_x$ about the $x$ axis in $CoSiF_6 \cdot 6H_2O$ at 140 K; curves are least-squares fit of the experimental data.

resolved at some other orientation. These features are very similar to that of $NiTiF_6 \cdot 6H_2O$ observed at 120 K ($<T_c$).[18] From the complete rotation pattern we have been able to determine fourteen EFG tensors (Table III) corresponding to seven $H_2O$ molecules per unit cell grouped into three $A$ type and four $B$ type (Table IV). Since the ratio of $A$- and $B$-type molecules is 2:1, there must be eight $A$-type molecules as there are four $B$-type molecules. This is because all the $^2$H lines for the $A$ type could not be resolved. According to this result the unit cell should contain 12 $H_2O$ molecules below the transition at $T_{c2}$. Thus it may be inferred that the second transition involves a cell doubling and is thus antiferrodistortive in nature. Moreover, the $^2$H NMR results of this phase is more compatible with the monoclinic symmetry.

Information about the hydrogen bond network in this phase is obtained from a comparison of the principal EFG tensors (Tables I and III) for the two phases, above and below the transition at $T_{c2}$ and is summarized as follows.

(1) Values of $e^2Qq/h$ indicate that the bond lengths are not altered appreciably.

(2) The O-H direction ($z_p$) of the $A$-type molecule changes very little whereas for $B$-type molecule this change is appreciable.

(3) The normal to the metal-oxygen-deuteron plane which is given by the $y_p$ direction, changes considerably. Consequently, the potential surfaces for all the O-H $\cdots$ F bonds are changed. The magnitudes of the changes, however, reveal that the transition is of displacive type and the deuteron in an O-H $\cdots$ F bond is located near the oxygen atom both above and below the transition at $T_{c2}$.

We have also determined complete EFG tensors for $CoTiF_6 \cdot 6H_2O$ below the transition at $T_{c2}$. Behavior of the hydrogen bond network is almost similar to that of $CoSiF_6 \cdot 6H_2O$. In case of $ZnTiF_6 \cdot H_2O$, the $^2$H lines have been detected below 160 K using a signal analyzer. A reasonable S/N ratio has been obtained by sweeping the magnetic field 20 times across the resonance frequency. The spectra reveal similar features as observed in case of $CoSiF_6 \cdot 6H_2O$ and $CoTiF_6 \cdot 6H_2O$ below the transition at $T_{c2}$. Since for $ZnTiF_6 \cdot H_2O$,[15] $T_{c2}=182$ K where the $^2$H lines are not detectable, we could not say about the nature of this transition. Thus, the $^2$H NMR results in $CoSiF_6 \cdot 6H_2O$, $CoTiF_6 \cdot 6H_2O$, and $ZnTiF_6 \cdot H_2O$ reveal that they transform from rhombohedral to monoclinic phase through an intermediate phase ($T_{c1} > T > T_{c2}$).

The existence of an intermediate phase in $NiTiF_6 \cdot 6H_2O$ has been predicted by Lichti[20] from the study of progression rate of the transition from the EPR of $Ni^{2+}$. A similar study of the deuterated analogue[21] however indicates that the range of the intermediate phase is very narrow (1.5 K). This is consistent with our observation of only one phase transition at $T_{c1}=129\pm2$ K in $NiTiF_6 \cdot 6H_2O$ from $^2$H NMR studies.[18] Recently, one such intermediate phase has also been detected from EPR studies[22] of $Mn^{2+}$-doped $MgSiF_6 \cdot 6H_2O$ with $T_{c1}=369$ K and $T_{c2}=296$ K. In this phase, the axial symmetry has been found to be retained which is in conformity with our observation. They further suggested from the resonance line shape that this intermediate phase is of incommensurate type with solitons appearing abruptly as a result of first-order transition. It is to be noted that previously $MgSiF_6 \cdot 6H_2O$ was considered to undergo structural phase transition[11] from $R\bar{3}$ ($Z=1$) to $P2_1/c$ ($Z=2$) at 296 K. Observation of the intermediate phase in the range 296–369 K, clearly supports our observation that some members of this isomorphous series, undergo structural transformation from $R\bar{3}$ to $P2_1/c$ symmetry through an intermediate phase. Moreover as in these compounds, the hydrogen atom in the O-H $\cdots$ F bond exists in an asymmetric double-well potential, there is a possibility of two successive phase transitions from the theoretical point of view as predicted by Blinc and Zeks.[23]

For $CoSiF_6 \cdot 6H_2O$, $CoTiF_6 \cdot 6H_2O$ and $ZnTiF_6 \cdot 6H_2O$, near the first transition at $T_{c1}$, the $(BF_6)^{2-}$ octahedra are known to undergo fast ($\gg 10^6$ Hz) reorientational motion.[24] This coupled with the observed fast flip motion of the $H_2O$ molecule results in a rather weak O-H $\cdots$ F bond. So these bonds would be less effective in communicating the effect of distortion of the water octahedra to the $(BF_6)^{2-}$ octahedra. In fact, the latter have been found to be regular below the transition at $T_{c1}$ from $^{19}$F NMR studies.[15] This could be a reason of small change in the crystal symmetry observed near the transition at $T_{c1}$ from $^2$H NMR studies.

The second transition at $T_{c2}$ occurs in a temperature region where both types of motions are comparatively slower ($\ll 10^6$ Hz). So in this region, O-H $\cdots$ F bonds are much stronger than they were near the transition at

$T_{c1}$. It is known[15] from $^{19}$F NMR of $ZnTiF_6 \cdot H_2O$ that the transition at $T_{c2}$ involves a tetragonal distortion of the $(TiF_6)^{2-}$ octahedra resulting in two types of fluorine atoms in the ratio 2:1. Consequently, the water octahedra suffer further distortion producing two types of water molecules, along with a drastic change in the lattice symmetry as observed from $^2$H NMR near the transition at $T_{c2}$.

TABLE III. Principal components and the direction cosines of the EFG tensors of deuterons in $CoSiF_6 \cdot 6H_2O$ at 140 K ($T < T_{c2}$).

| | | $e^2Qq_{ii}/h$ | Direction cosines with respect to crystrallographic axes | | |
|---|---|---|---|---|---|
| Tensor | Deuteron | (kHz) | $x$ | $y$ | $z$ |
| | | | Type $A$ | | |
| I | $D_1$ | 110.1 | 0.2176 | −0.9696 | −0.1116 |
| | | 137.1 | 0.9395 | 0.2391 | −0.2452 |
| | | −247.2 | 0.2644 | −0.0515 | 0.9630 |
| II | $D_3$ | 106.4 | −0.7107 | 0.6530 | −0.2617 |
| | | 144.1 | 0.6941 | 0.7114 | −0.1099 |
| | | −250.5 | −0.1144 | 0.2597 | 0.9589 |
| III | $D_5$ | 118.7 | −0.7107 | 0.6530 | −0.2617 |
| | | 130.8 | 0.6941 | 0.7114 | −0.1099 |
| | | −249.5 | −0.1144 | 0.2597 | 0.9589 |
| IV | $D_2$ | −102.8 | −0.1854 | −0.0901 | 0.9785 |
| | | −130.9 | 0.0693 | 0.9921 | 0.1044 |
| | | 238.7 | −0.9802 | 0.0872 | −0.1776 |
| V | $D_4$ | −102.5 | −0.0255 | 0.2116 | 0.9770 |
| | | −128.9 | 0.8255 | −0.5467 | 0.1400 |
| | | 231.4 | 0.5638 | 0.8101 | −0.1607 |
| VI | $D_6$ | −103.7 | 0.3175 | −0.0283 | 0.9478 |
| | | −135.2 | 0.8524 | 0.4464 | −0.2723 |
| | | 238.9 | 0.4154 | −0.8944 | −0.1658 |
| | | | Type $B$ | | |
| I′ | $D_1'$ | 112.4 | 0.0236 | 0.9993 | 0.0290 |
| | | 127.6 | 0.9567 | −0.0142 | −0.0291 |
| | | −240.0 | 0.2901 | −0.0346 | 0.9504 |
| I″ | $D_1''$ | 107.2 | 0.8968 | 0.3816 | 0.2237 |
| | | 129.5 | −0.3489 | 0.9211 | −0.1724 |
| | | −236.7 | −0.2719 | 0.0765 | 0.9593 |
| II′ | $D_3'$ | 104.7 | 0.8133 | 0.5415 | 0.2127 |
| | | 135.6 | 0.5773 | −0.7965 | −0.1798 |
| | | −240.3 | −0.0721 | −0.2691 | 0.9604 |
| III′ | $D_5'$ | 113.0 | 0.8867 | −0.4618 | 0.0234 |
| | | 127.8 | 0.4478 | 0.8452 | −0.2915 |
| | | −240.8 | 0.1148 | 0.2689 | 0.9563 |
| IV′ | $D_2'$ | −103.7 | −0.1643 | 0.2631 | 0.9504 |
| | | −131.2 | 0.4631 | 0.3714 | −0.1621 |
| | | 234.9 | −0.8709 | 0.4135 | −0.2655 |
| IV″ | $D_2''$ | −92.4 | 0.2517 | −0.1404 | 0.9575 |
| | | −138.0 | −0.2846 | 0.9349 | 0.2119 |
| | | 230.4 | 0.9249 | 0.3259 | −0.1954 |
| V′ | $D_4'$ | −93.5 | −0.0017 | 0.2949 | 0.9555 |
| | | −136.1 | 0.6672 | 0.7114 | −0.2208 |
| | | 229.6 | 0.7449 | 0.6379 | −0.1955 |
| VI′ | $D_6'$ | −105.1 | 0.1751 | −0.2729 | 0.9459 |
| | | −131.6 | 0.9819 | −0.0223 | −0.1881 |
| | | 236.7 | 0.0724 | 0.9618 | 0.2640 |

TABLE IV. Electric quadrupole coupling constant $e^2Qq/h$, asymmetry parameter $\eta$ of deuterons and the average value of the angle $\phi_z$ between the $z$ principal axes of two deuterons belonging to $H_2O$ molecules of $CoSiF_6 \cdot 6H_2O$ at $T = 140$ K ($T < T_{c2}$).

| Assignment | | $e^2Qq/h$ (kHz) | Asymmetry parameter $\eta$ | Average $\phi_z$ (deg) |
|---|---|---|---|---|
| | | Type $A$ | | |
| $O_I$ | $D_1$ | $-247.2 \pm 2.0$ | $0.109 \pm 0.02$ | $113 \pm 3$ |
| | $D_2$ | 238.7 | 0.121 | |
| $O_{II}$ | $D_3$ | $-250.5$ | 0.150 | |
| | $D_4$ | 231.4 | 0.114 | |
| $O_{III}$ | $D_5$ | $-249.5$ | 0.050 | |
| | $D_6$ | 238.9 | 0.121 | |
| | | Type B | | |
| $O_{I'}$ | $D_{1'}$ | $-240.0$ | 0.036 | $113 \pm 3$ |
| | $D_{2'}$ | 235.0 | 0.111 | |
| $O_{I'''}$ | $D_{1''}$ | $-236.7$ | 0.094 | |
| | $D_{2'''}$ | 230.4 | 0.119 | |
| $O_{II''}$ | $D_{3'}$ | $-240.3$ | 0.113 | |
| | $D_{4'}$ | 229.6 | 0.118 | |
| $O_{III'}$ | $D_{5'}$ | $-240.8$ | 0.062 | |
| | $D_{6'}$ | 236.7 | 0.111 | |

## IV. CONCLUSION

(i) For the first time evidence of two successive phase transitions in the range 100–300 K for $CoSiF_6 \cdot 6H_2O$, $CoTiF_6 \cdot 6H_2O$ and $ZnTiF_6 \cdot H_2O$ have been obtained. The results clearly indicate that the transition from $R\overline{3}$ ($Z=1$) to $P2_1/c$ ($Z=2$) symmetry takes place through an intermediate phase ($T_{c1} > T > T_{c2}$), whose crystal structure is yet to be determined. For $NiTiF_6 \cdot 6H_2O$, the temperature range for this intermediate phase may be very narrow and thus could not be observed.

(ii) During the transition at $T_{c1}$, though the crystal is distorted, the equivalency of six $H_2O$ molecules is retained and the unit cell still remains unimolecular. The second transition at $T_{c2}$ in the above three compounds and the only transition in $NiTiF_6 \cdot 6H_2O$ is accompanied by a drastic change in crystal symmetry, which destroys the equivalency of the water molecules.

(iii) The present work throws light on the hydrogen bond network in different crystal phases. During the transition at $T_{c1}$, the shape of the potential well of an O-H $\cdots$ F bond, is altered significantly while the O-H directions are affected uniformly. However, during the transition at $T_{c2}$ both change drastically, particularly the change in O-H directions in non-uniform, leading to a drastic change in crystal symmetry accompanied by a cell doubling.

## ACKNOWLEDGMENTS

We wish to thank Dr. S. Bhattacharya for his generous help in the computational work and Mrs. A. Basu for her involvement in the initial phase of the work.

---

[1] M. Majumder and S. K. Datta, J. Chem. Phys. **42**, 418 (1965).

[2] B. Ghosh, N. Chatterjee, A. N. Das, and A. Chatterjee, J. Phys. C **12**, 3283 (1979).

[3] P. Chowdhury, A. N. Das, N. Chatterjee, and B. Ghosh, Indian J. Pure Appl. Phys. **20**, 241 (1982).

[4] M. Karnezos and S. A. Friedberg, J. Appl. Phys. **49**, 1382 (1978).

[5] U. Volland, S. Hosl, H. Spiering, I. Dezsi, T. Kemeny, and D. L. Nagy, Solid State Commun. **27**, 49 (1978).

[6] R. S. Rubins, B. C. Griffin, and R. Burris, J. Chem. Phys. **64**, 3349 (1976).

[7] T. E. Jenkins and J. Lewis, J. Raman Spectrosc. **8**, 111 (1979).

[8] T. E. Jenkins and J. Lewis, Spectrochim. Acta, Part A **37**, 47 (1980).

[9] P. Chowdhury, B. Ghosh, M. B. Patel, and H. D. Bist, J. Phys. C **17**, 5827 (1984).

[10] R. W. L. Wyckoff, *Crystal Structures* (Wiley, New York, 1964), Vol. 2, p. 203.

[11] S. Syoyama and K. Osaki, Acta Crystallogr. Sect. B **28**, 2626 (1975).

[12] E. Kodera, A. Torri, K. Osabi, and T. Watanabe, J. Phys. Soc. Jpn. **32**, 863 (1972).

[13] G. Jayaram and S. Sastry, Chem. Phys. Lett. **77**, 314 (1981).

[14] R. S. Rubins, Chem. Phys. Lett. **28**, 273 (1974).

[15] M. L. Afanasyev, A. F. Lybzikov, V. V. Menshikov, and E. P. Zeer, Chem. Phys. Lett. **60**, 279 (1979).

[16] M. H. Cohen and R. Reif, *Solid State Physics*, edited by F. Seitz and D. Turnbull (Academic, New York, 1957), Vol. 3.

[17] M. Bose, A. Ghoshray, A. Basu, and K. Roy, J. Phys. C **12**, L771 (1979).

[18] M. Bose, K. Roy, and A. Ghoshray, J. Phys. C **16**, 645 (1983); **17**, 5277 (1984); **17**, L757 (1984).

[19] G. Soda and T. Chiba, J. Chem. Phys. **50**, 439 (1969).

[20] R. L. Lichti, J. Chem. Phys. **78**, 7323 (1983).

[21] R. L. Lichti, Chem. Phys. Lett. **105**, 228 (1984).

[22] A. M. Ziatdinov, V. G. Kuryavyi, and R. Davidovich, Fiz. Tverd. Tela (Leningrad) **27**, 2152 (1985) [Sov. Phys.—Solid State **27**, 1288 (1985)].

[23] R. Blinc and B. Zeks, Adv. Phys. **21**, 693 (1972).

[24] S. M. Skjaeveland and I. Svare, Phys. Scr. **10**, 273 (1974).